(Received 11 December 2023, Accepted 26 January 2024, Scheduled 8 February 2024)

Dual Split Ring Resonator Based Reconfigurable Reflective Metasurface for Linear-to-Linear Polarization Conversion

Kinatingal Neema* and Deepti Das Krishna

Center for Research in ElectroMagnetics and Antennas (CREMA), Department of Electronics
Cochin University of Science and Technology, Kochi, India

ABSTRACT: A metasurface that can be reconfigured for the conversion of linear-to-linear polarization has been designed, fabricated, and verified. It consists of dual co-centric split-ring resonators (SRRs), each of which has a pair of splits. It is specifically engineered to function in two reflection modes, one with polarization conversion and the other without. The unit cell achieves reconfiguration by utilizing two PIN diodes. Conversion of linear polarization to its perpendicular counterpart is achieved while the diodes are in the OFF state. When the PIN diodes are turned ON, full reflection without polarization conversion occurs. The proposed meta-surface operates over the 6.03–10.5 GHz frequency range. A 42×42 unit cell array is fabricated, and the results are experimentally verified. An FR4 substrate is used with copper ground plane on one side. The polarization conversion is measured and compared with simulation results for various incident angles. A Polarization Conversion Ratio (PCR) of $\geq 90\%$ is achieved for incident angles up to 30°, with simulation and measured results showing good agreement.

1. INTRODUCTION

Despite the fact that 5G coverage is not yet fully established, the research community has already proposed the sixth generation (6G) of mobile communication. There are various technologies that can be employed to achieve this goal, such as Reconfigurable Intelligent Surfaces/Intelligent Reflecting Surfaces (RIS/IRSs), Visible Light Communications (VLCs), and electromagnetic-orbital angular momentum [1]. The concept of IRS is a promising technology for 6G wireless communication [2], because it is reported to exhibit the ability to control various properties of electromagnetic waves, such as their phase, amplitude, frequency, and polarization [3]. This is made possible by utilizing two-dimensional metamaterials called metasurfaces, which are made up of subwavelength metallic or dielectric structures [4, 5]. Metasurfaces offer a less bulky, simpler and lower loss alternative to metamaterials. In fact, metasurfaces have been used to manipulate wavefronts, convert polarizations, control radiation, and concentrate energy with great success over the past decade [6]. Split Ring Resonators (SRRs) are a popular choice for constructing metasurfaces, which have received significant research interest during the last decade for their negative permeability which is not attainable with ordinary materials. The resonance frequency of an SRR is determined by its dimensions, which can be adjusted to tune from microwave to terahertz and even visible frequencies [7]. Moreover, the SRR's anisotropic structure enables polarization conversion. Spiral split ring resonators [8], S-shaped split ring resonators [9], twisted split ring resonators [10] are some such SRRs.

Various studies have reported metasurface based polarization converters which are primarily composed of a metallic pattern printed over a dielectric, backed by a ground plane. Depending on the presence and absence of the ground plane, these converters can be reflective and transmissive, respectively [11–15]. However, developing an active polarization converter that operates in transmissive mode is a challenging task. This is mainly because, unlike reflective mode polarization converters, it is impossible to isolate the bias network from the incoming waves due to the absence of the ground plane. This significantly affects the converter's efficiency. Additionally, minimizing reflection and insertion loss throughout the entire operating frequency range is a major challenge [15]. In a reflective-type polarization converter, the biasing network is isolated by the ground plane, so there will be no interaction between the bias lines and the incoming waves. Therefore, the polarization conversion efficiency is higher in the reflective type compared with the transmission type [16].

In [17], a reflective-type metasurface polarization converter is reported to have dual co-centric split ring resonators. It exhibits linear-to-linear polarization conversion, and the polarization of the reflected wave depends on the orientation of the splits. If we are able to selectively introduce the splits, a reconfigurable linear-to-linear polarization converter can be achieved [18]. In this paper, we have incorporated RF switches in the outer SRR, which enables us to switch between two orthogonal polarizations. When the PIN diodes are in OFF state, they serve as a linear cross-polarization converter (x-polarized wave incident is converted to a y-polarized wave and vice versa). When the PIN diodes are in ON state, they function as metal-like reflectors (x or y-polarized incident wave continues to be reflected as an x-polarized or y-polarized wave).

* Corresponding author: Kinatingal Neema (neemak@cusat.ac.in).

Dimension	Value (mm)
L	5.1
M	2.5
g	1
s	0.45
r	0.8
h	3.2
P	7

TABLE 1. Optimized values.

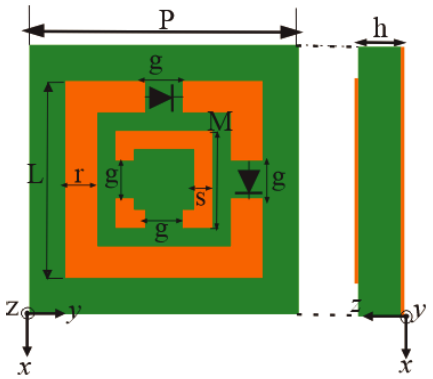

FIGURE 1. Schematic of the proposed unit cell.

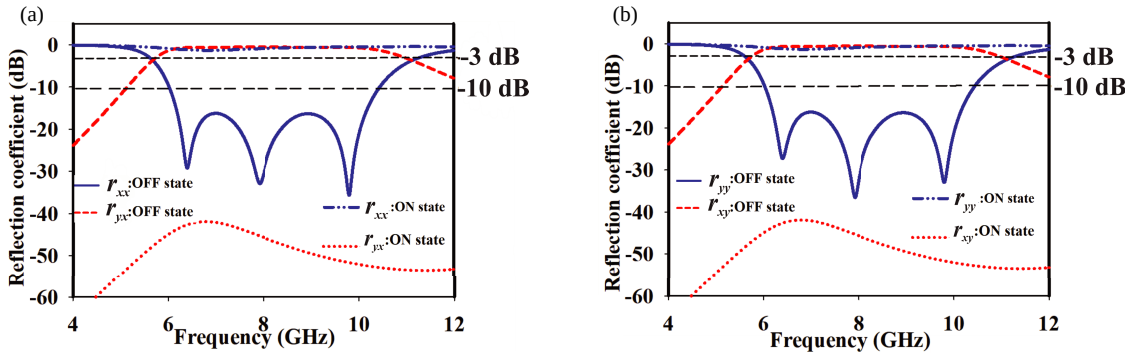

FIGURE 2. Simulated co- and cross-polarized reflection coefficients for an (a) x-polarized and (b) y-polarized incident wave, when PIN diodes are ON and OFF, respectively.

2. PROPOSED DESIGN

The schematic of the unit cell and its dimensions are shown in Fig. 1 and Table 1, respectively. Here, the SRR has two splits orthogonal to each other, where P is the periodicity. An FR4 substrate that is 3.2 mm thick with a relative permittivity of 4.4 and a loss tangent of 0.02 is used here, and is backed by a metal plane since it is designed as a reflective-type polarization converter. Two PIN diodes, per unit cell, are loaded on the the outer SRR. For the given gap length g, the PIN diode HPND-4005 [19] is modelled as a 4.7 Ω resistor in its ON state and as a 0.017 pF capacitor in the OFF state.

To analyze the results, we need to define the reflection coefficients of cross-polarized and co-polarized reflected waves from this metasurface. Cross-polarized reflection coefficient $r_{yx}(r_{xy})$ is defined as the ratio of the reflected y-polarized (x-polarized) electric field to the incident x-polarized (y-polarized) electric field [13]

$$r_{yx} = E_y^{Ref}/E_x^{Inc}; \quad r_{xy} = E_x^{Ref}/E_y^{Inc} \tag{1}$$

Ideally, in the case of complete polarization conversion, the magnitude of r_{yx} and r_{xy} approaches 0 dB. Similarly, co-polarized reflection coefficients (r_{xx}, r_{yy}) can also be defined as:

$$r_{xx} = E_x^{Ref}/E_x^{Inc}; \quad r_{yy} = E_y^{Ref}/E_y^{Inc} \tag{2}$$

In the case of a good polarization conversion, the magnitude of r_{xx} and r_{yy} approaches values < -10 dB. In order to quantify the linear-to-linear polarization conversion, another term called Polarization Conversion Ratio (PCR), which is used to define polarization conversion efficiency, is also defined.

$$\text{PCR}_x = r_{yx}^2/(r_{xx}^2 + r_{yx}^2); \quad \text{PCR}_y = r_{xy}^2/(r_{yy}^2 + r_{xy}^2) \tag{3}$$

where PCR_x is for the x-polarized incident wave and PCR_y for the y-polarized incident wave. It quantifies how effectively a metasurface can rotate the polarization from one orthogonal plane to another.

For simulating the performance of the metasurface using 3D simulation tool, a master-slave boundary condition is used to represent the infinite repetition of the unit cell with a Flouquet port excitation. Fig. 2(a) and Fig. 2(b) indicate the r_{xx}, r_{yx}, r_{yy}, and r_{xy} in the case of a normal incidence for the ON and OFF conditions of the PIN diode.

Within the frequency band of 6.03 to 10.5 GHz, co-polarization reflection coefficients are observed to be less than -10 dB. At the same time, r_{yx} and r_{xy} remain above -3 dB between 5.76 and 10.93 GHz, confirming a strong cross-polarization and a relatively weak co-polarization. When the PIN diodes are switched ON, the co-polarization reflection coefficient shifts to 0 dB, and the cross-polarization reflection coefficients are < -40 dB in the 4–12 GHz frequency range. Hence, this confirms the reconfigurable performance of the proposed metasurface controlled by the state of the PIN diodes.

Figures 3(a) and 3(b) show the PCR values for PIN diodes in the OFF state when being subjected to an x-polarized and

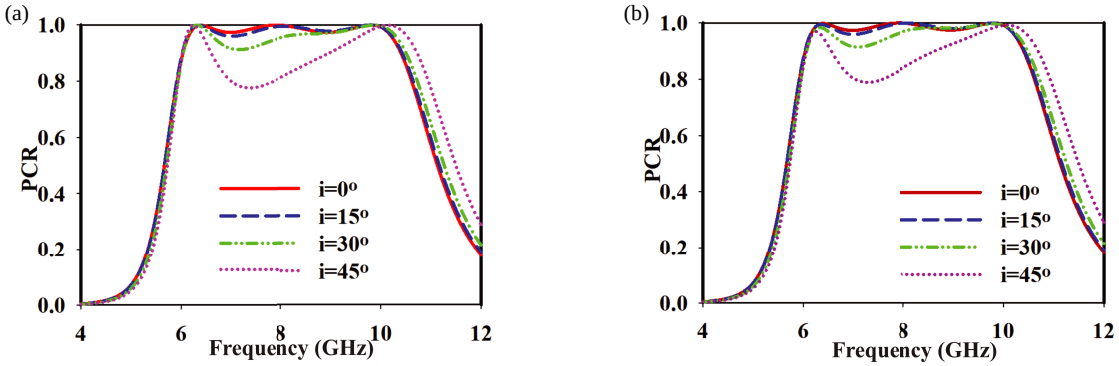

FIGURE 3. PCR for (a) the x-polarized and (b) the y-polarized incident wave at different incident angles 'i' while keeping PIN diodes OFF.

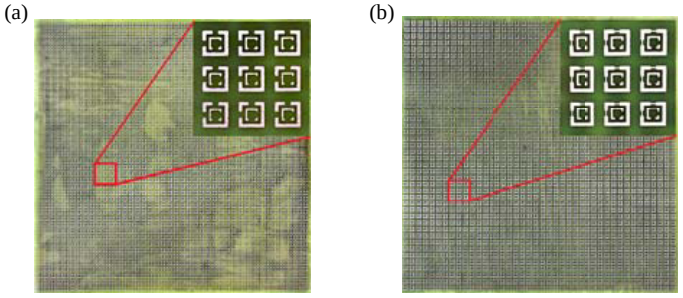

FIGURE 4. (a) OFF state. (b) ON state.

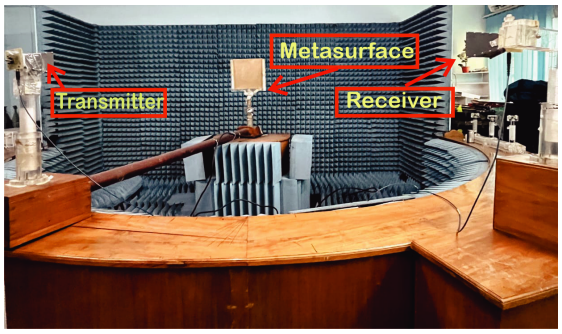

FIGURE 5. Measurement setup.

a y-polarized incident wave respectively at different angles of incidence 'i'. The results indicate a PCR of $\geq 90\%$ for angles between $0°$ and $30°$. Beyond this, the PCR value starts to decrease. This degradation could be attributed to several reasons. As the angle of incidence increases, the effective properties of the metasurface by virtue of its anisotropy, spatial distribution of incident wave across the metasurface, and the effective path length through the metasurface can vary depending on the specific design and characteristics of the metasurface leading to deterioration in the performance. Hence, we can conclude that the proposed metasurface is capable of linear-to-linear polarization conversion for incident angles up to $30°$ during the OFF state of the PIN diodes. In the ON state, it functions as a normal perfect reflector.

3. RESULTS

To validate the simulation studies, the metasurface based on the proposed unit cell is fabricated and measured, as shown in Fig. 4. The metasurface is composed of 42×42 unit cells with an overall size of 30.5 cm $\times$ 30.5 cm and is fabricated on a 3.2 mm thick FR4 substrate with a copper coating on the reverse side.

Here, the switching action is emulated by using open and short strips across the splits, as shown in Fig. 4(a) and Fig. 4(b), respectively. The arch-type measurement testing system in a semi-anechoic chamber with a bistatic measurement setup is shown in Fig. 5, allowing an incident angle variation from $0°$ to $90°$. Two horn antennas operating over 2–18 GHz, along with R&S ZVB20 vector network analyzer are utilized. To accurately calibrate the system, a metal sheet that matches the size of the proposed metasurface is used.

Figures 6(a) and (b) show the measured co- and cross-polarized reflection coefficients at normal incidence, along with simulated values when PIN diodes are in ON and OFF states. It is worth noting that the measured performance matches the predicted one, where cross-polarized reflection dominates when the switch is OFF, and co-polarized reflection dominates when the switch is ON in the frequency range of 6.04 to 10.5 GHz. The simulation results show that, when the PIN diodes are in ON state, a complete reflection without polarization conversion is observed. But in measured results, some amount of cross-polarized reflection (still much less than co-polarized reflection) is observed. Hence, the proposed metasurface can function as a perfect reflector both with or without $90°$ polarization rotation, depending on the state of the PIN diodes.

In our investigation, we examined the polarization conversion efficiency by varying angles of incidence ($+90°$ to $-90°$). The outcomes of this analysis are presented in Fig. 7, and it is evident that the polarization conversion property tends to decline with an increase in the incident angle, which is consistent with the simulation results. According to the findings, the polarization conversion property is deemed satisfactory when it comes to incident angles of up to $\pm 30°$. Manufacturing tolerances and measurement apparatus irregularities can be the reason for the deviations between measured and simulated results.

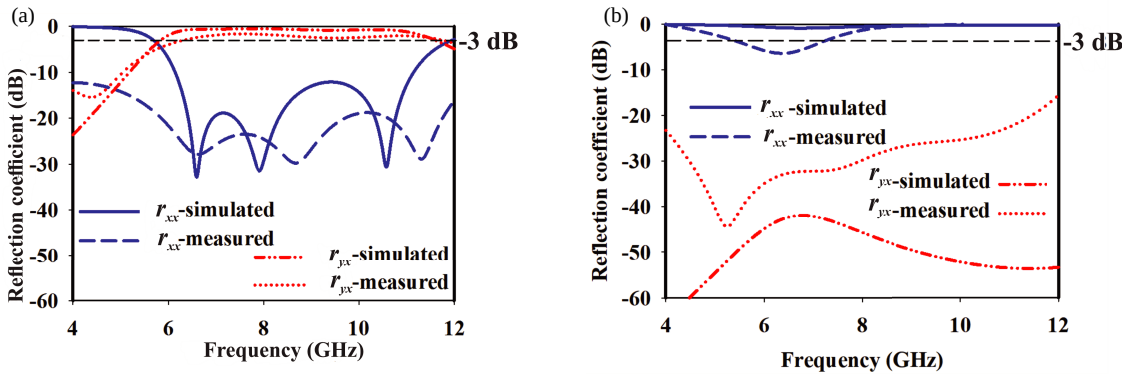

FIGURE 6. Comparison between measured value of co-and cross polarization reflection coefficient along with the simulated results when PIN diodes are in (a) OFF State, (b) ON State at normal incidence.

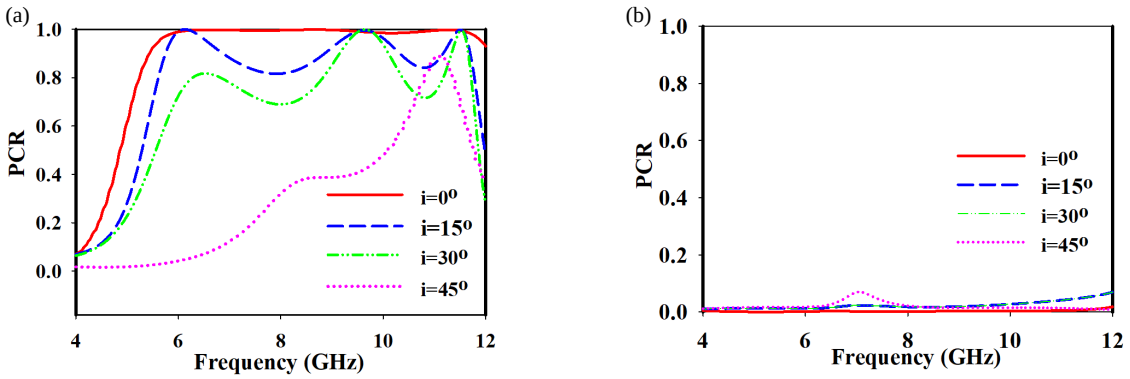

FIGURE 7. PCR value When the PIN diodes are in (a) OFF state and in (b) ON state.

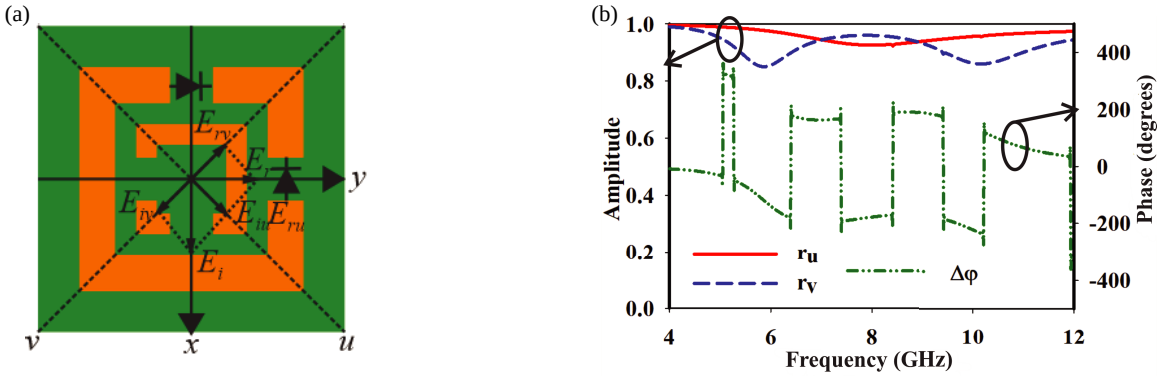

FIGURE 8. (a) Incident electric field (x-polarized) represented in terms of u and v orthogonal vectors. (b) Simulated amplitude and phase difference of reflection coefficients, r_u and r_v.

4. THEORETICAL ANALYSIS

A theoretical model is explored to gain a better understanding of the polarization conversion process. This model is used to interpret the results along with physical insights. Assume that an x-polarized linearly polarized wave $\vec{E} = \hat{x}E_0e^{i(\omega t-kz)}$ propagating along the z-axis is incident on the proposed metasurface, where E_0 is the amplitude of the incident electric field, k the wave vector, and ω the angular frequency. The incident electric field can be written in terms of its two orthogonal components along the u and v axes, as shown in Fig. 8(a), as:

$$\vec{E}_i = \hat{u}E_{iu}e^{i\phi} + \hat{v}E_{iv}e^{i\phi} = \hat{u}\,\frac{E_0}{\sqrt{2}}\,e^{i\phi} - \hat{v}\,\frac{E_0}{\sqrt{2}}\,e^{i\phi} \quad (4)$$

where $\phi = \omega t - kz$, the subscripts i and r represent the incident and reflected electric fields, and u and v represent orthogonal directions. The electric field upon reflection from the metasurface can be expressed as:

$$\vec{E}_r = \hat{u}E_{ru}e^{i\phi'} + \hat{v}E_{rv}e^{i\phi'} = \left(\hat{u}r_uE_{iu} + \hat{v}r_vE_{iv}e^{i\Delta\psi}\right)e^{i\phi'} \quad (5)$$

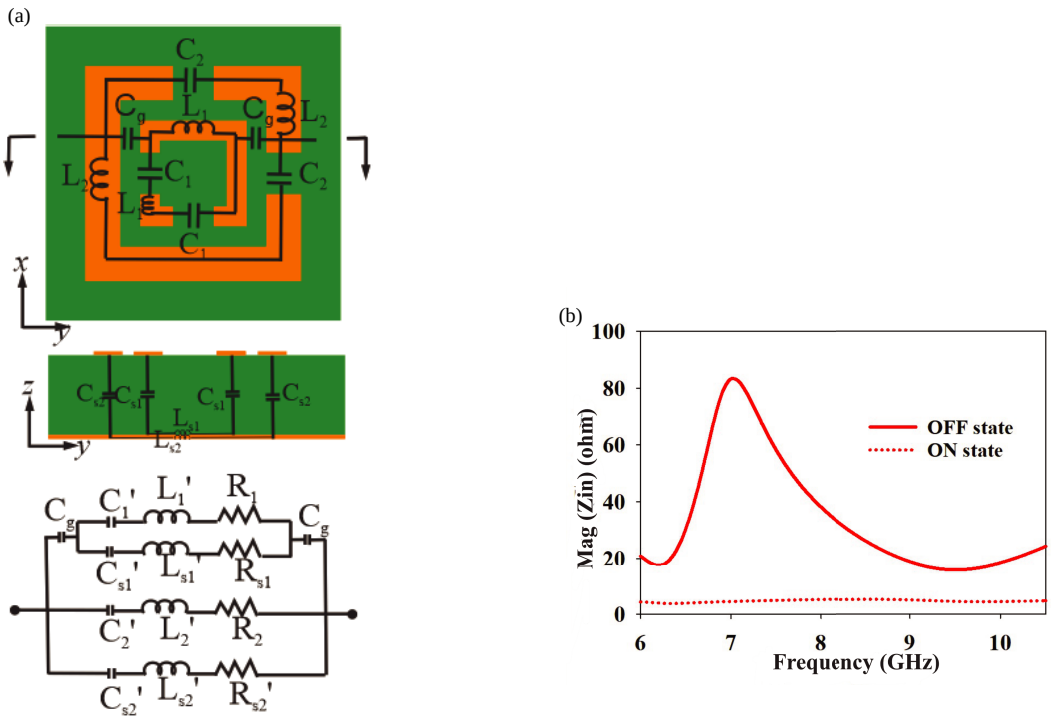

FIGURE 9. (a) The PCM's equivalent circuit and simplified circuit. (b) Impedance vs. frequency graph in the ON state.

where $\phi' = \omega t + kz$ and r_u & r_v are the reflection coefficients along the *u* & *v* axes, respectively, and $\Delta\psi$ represents the phase difference between E_{ru} and E_{rv} due to the anisotropy of the metasurface. If $r_u \approx r_v$ and $\Delta\psi = \pm 180°$, the vector sum of E_{ru} & E_{rv} will be along y direction as shown in Fig. 8(a), which indicates that the reflected wave is y-polarized. This is verified in Fig. 8(b), where the amplitude and phase difference of reflection coefficients r_u and r_v is plotted for the case when polarization conversion is happening. As we can observe, over the frequency range 6.02 to 10.53 GHz, the amplitude of r_u and r_v is almost the same and ≈ 1. In the same frequency range, the phase difference $\Delta\psi$ between the reflection coefficients is $\pm 180°$, which clearly indicates an orthogonal polarization rotation of the reflected wave.

Next, we have tried to explain the performance of the proposed reconfigurable metasurface in terms of an equivalent circuit. For example, when a y-polarized wave is incident on the unit cell, a current will be induced in the y-direction. The metal lines on the unit cell can be represented as inductors while the splits in the individual SRRs and the gap between the two SRRs can be represented as capacitors. The circuit also includes four resistors to account for the internal resistance of capacitors, dielectrics, and inductors. The simplified equivalent circuit is shown in Fig. 9(a), which is simulated in ADS, and the optimized component values are given in Table 2.

The capacitor C_2 (0.017 pF) represents the PIN diode in its OFF state as mentioned in Section 2. To represent the switch in the ON state, this C_2 is replaced by a resistor of 4.7 Ω. Simulated impedance values show a change in impedance for the two states as shown in Fig. 9(b). The capacitor C_2 (0.017 pF) represents the capacitance across the diode replaced by 4.7 Ω resistor

TABLE 2. Optimized values.

Component	Value	Component	Value
$L_1' = L_1/2$	0.0081 nH	$L_2' = L_2/2$	0.083 nH
L_{s1}'	1.35 nH	L_{s2}'	5.92 nH
$C_1' = 2C_1$	0.04 pF	$C_2' = 2C_2$	0.04 pF
$C_{s1}' = C_{b1}/2$	0.25 pF	$C_{s2}' = C_{b2}/2$	0.11 pF
C_g	2.17 pF	R_1	0.041 Ω
R_2	0.46 Ω	R_{s1}	14.84 Ω
R_{s2}'	19.91 Ω		

in the case of ON state of the PIN diode as modelled in the simulation. In the ON state, the impedance for current flowing in the y direction is minimum which means that the y-polarized wave will be reflected from the structure as in the case of a metal reflector. In the OFF state, the impedance value increases which means that an x-polarized wave will be reflected [20].

To further explain the mechanism of polarization conversion, Fig. 10 shows surface current distributions at three resonant frequencies (6.416 GHz, 7.872 GHz, and 9.904 GHz) on the split ring resonators and the bottom ground plane. At 6.416 GHz and 7.872 GHz, the currents are antiparallel to each other as shown in Figs. 10(a) and 10(b), which represent a magnetic resonance. At 9.904 GHz, the currents on the top SRRs are parallel and antiparallel with the currents on the ground plane which represents an electric resonance and magnetic resonance respectively at the same time as shown in Fig. 10(c). The surface current distribution of the proposed metasurface hence reveals its ability to excite both electric and magnetic resonances [21].

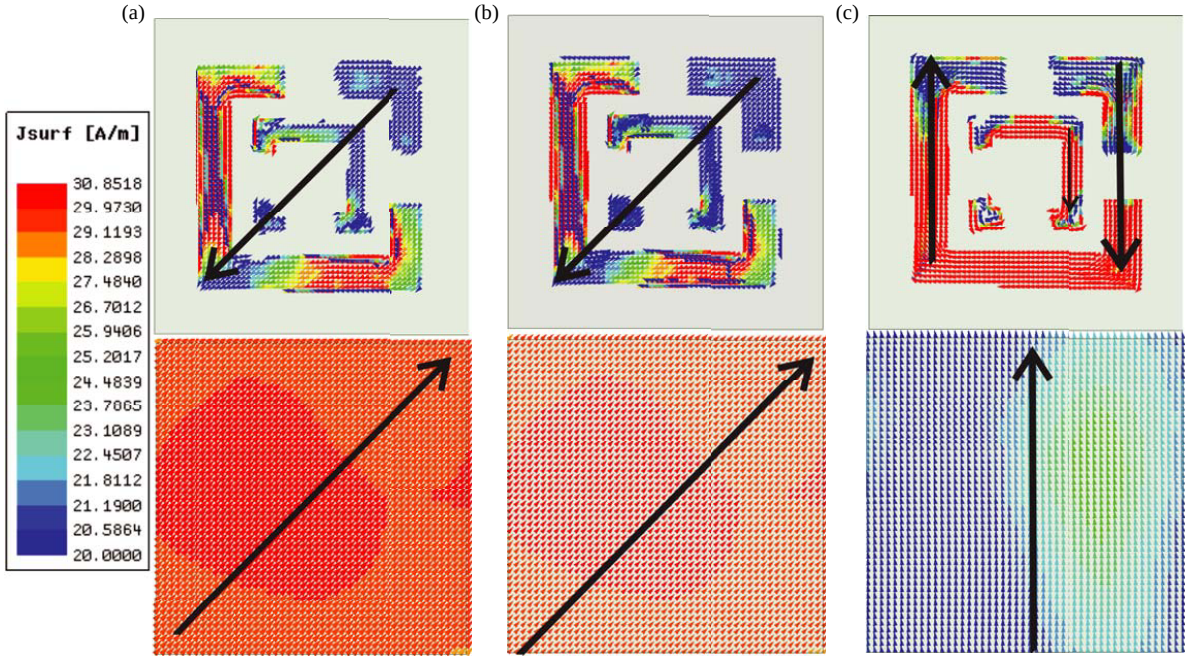

FIGURE 10. Surface current distribution at (a) 6.416 GHz, (b) 7.872 GHz and (c) 9.904 GHz.

TABLE 3. Comparison with previous related works.

Refs.	R	T (mm)	RBW (%)	A.S	N.PD
[23]-2022	No	$0.036\lambda_c$	5	80° BW decreases	Nil
[24]-2023	No	$0.108\lambda_c$	44.7 & 9.7	Not given	Nil
[25]-2020	No	$0.104\lambda_c$	79.2	Not given	Nil
[20]-2018	Yes	$0.0714\lambda_c$	38.6	30° PCR > 80%	2
[22]-2022	Yes	$0.23\lambda_c$	81	Not given	2
[18]-2022	Yes	$0.0876\lambda_c$	61	30°	4
Proposed work	Yes	$0.0852\lambda_c$	54.5	30° PCR > 90%	2

R: reconfigurable, T: thickness, RBW: relative bandwidth, A.S: angular stability, λ_c: wavelength at the centre frequency, N.PD: No. of PIN diodes

The performance of the proposed design is compared with the previously published literature in Table 3. It is observed that the suggested SRR-based metasurface for polarization conversion performs broadband and has a design that is simpler and has compact construction. Additionally, the proposed metasurface exhibits a PCR value of 90% up to 30° angle of incidence.

5. CONCLUSION

A reconfigurable reflective metasurface for linear-to-linear polarization conversion employing PIN diodes has been developed. It can flip between linear to linear polarization rotation mode and non-polarization rotation reflection mode. Over the frequency range of 6.03–10.5 GHz, the PCR value is above 90% in the conversion mode at normal incidence. In the reflection mode, co-polarized reflection coefficients are ≥ -1 dB in the frequency range of 4–12 GHz. The surface is fabricated, and results are verified experimentally. The measured results confirm the simulation studies. Applications for the suggested polarization converter include communication systems, stealth technologies, RCS reduction, and intelligent reflecting surfaces (IRS).

ACKNOWLEDGEMENT

The authors would like to thank RUSA 2.0 Major project T4H for the support.

REFERENCES

[1] Porambage, P., G. Gür, D. P. M. Osorio, M. Liyanage, A. Gurtov, and M. Ylianttila, "The roadmap to 6G security and privacy," *IEEE Open Journal of the Communications Society*, Vol. 2, 1094–1122, 2021.

[2] Hassouna, S., M. Jamshed, J. Rains, J. Kazim, M. Ur-Rehman, M. Abualhayja *et al.*, "A survey on reconfigurable intelligent surfaces: Wireless communication perspective," *IET Communications*, Vol. 17, No. 5, 497–537, 2023.

[3] Basar, E., M. D. Renzo, J. D. Rosny, M. Debbah, M.-S. Alouini, and R. Zhang, "Wireless communications through reconfigurable intelligent surfaces," *IEEE Access*, Vol. 7, 116 753–116 773, Aug. 2019.

[4] Liu, Y. and X. Zhang, "Metamaterials: A new frontier of science and technology," *Chemical Society Reviews*, Vol. 40, No. 5, 2494–2507, 2011.

[5] Engheta, N. and R. W. Ziolkowski, *Metamaterials: Physics and Engineering Explorations*, 1st ed., John Wiley & Sons, 2006.

[6] Hu, J., S. Bandyopadhyay, Y.-H. Liu, and L.-Y. Shao, "A review on metasurface: From principle to smart metadevices," *Frontiers in Physics*, Vol. 8, 586087, 2021.

[7] Yang, T., X. Liu, C. Wang, Z. Liu, J. Sun, and J. Zhou, "Polarization conversion in terahertz planar metamaterial composed of split-ring resonators," *Optics Communications*, Vol. 472, 125897, Oct. 2020.

[8] Yang, T., X. Liu, C. Wang, F. Wang, and J. Zhou, "High-efficiency cross-polarization conversion metamaterial using spiral split-ring resonators," *AIP Advances*, Vol. 10, No. 9, 095210, Sep. 2020.

[9] Li, E., X. J. Li, B.-C. Seet, A. Ghaffar, and A. Aneja, "A metasurface-based LTC polarization converter with S-shaped split ring resonator structure for flexible applications," *Sensors*, Vol. 23, No. 14, 6268, Jul. 2023.

[10] Cheng, Y., Y. Nie, X. Wang, and R. Gong, "An ultrathin transparent metamaterial polarization transformer based on a twist-split-ring resonator," *Applied Physics A*, Vol. 111, 209–215, 2013.

[11] Fei, P., W. Guo, W. Hu, Q. Zheng, X. Wen, X. Chen, and G. A. E. Vandenbosch, "A transmissive frequency-reconfigurable cross-polarization conversion surface," *IEEE Antennas and Wireless Propagation Letters*, Vol. 21, No. 5, 997–1001, May 2022.

[12] Li, W., S. Xia, B. He, J. Chen, H. Shi, A. Zhang, Z. Li, and Z. Xu, "A reconfigurable polarization converter using active metasurface and its application in horn antenna," *IEEE Transactions on Antennas and Propagation*, Vol. 64, No. 12, 5281–5290, Dec. 2016.

[13] Li, W., S. Xia, H. Shi, G. Dong, A. Zhang, Z. Li, and Z. Xu, "Design of a reconfigurable polarization converter based on RF switches," in *2017 IEEE International Symposium on Antennas and Propagation & USNC/URSI National Radio Science Meeting*, 885–886, San Diego, CA, USA, Jul. 2017.

[14] Pramanik, S., S. C. Bakshi, D. Mitra, and C. Koley, "Design and analysis of a reconfigurable polarization conversion metasurface," in *2019 IEEE Indian Conference on Antennas and Propogation (InCAP)*, 1–4, Ahmedabad, India, 2019.

[15] Pramanik, S., S. C. Bakshi, D. Mitra, and C. Koley, "PIN diodes based bi-functional metasurface with polarization conversion and full reflection characteristics," in *2021 IEEE Indian Conference on Antennas and Propagation (InCAP)*, 595–597, Jaipur, Rajasthan, India, 2021.

[16] Wu, Z., Y. Ra'di, and A. Grbic, "Tunable metasurfaces: A polarization rotator design," *Physical Review X*, Vol. 9, No. 1, 011036, Feb. 2019.

[17] Khan, M. I., Q. Fraz, and F. A. Tahir, "Ultra-wideband cross polarization conversion metasurface insensitive to incidence angle," *Journal of Applied Physics*, Vol. 121, No. 4, 2017.

[18] Neema, K., A. Suresh, and D. D. Krishna, "Re-configurable metasurface for polarization conversion," in *2022 IEEE 19th India Council International Conference (INDICON)*, Nov. 2022.

[19] Jose, S., "HPND-4005 beam lead PIN diode, Datasheet," *Avago Technologies, CA*, 2006.

[20] Sun, S., W. Jiang, S. Gong, and T. Hong, "Reconfigurable linear-to-linear polarization conversion metasurface based on PIN diodes," *IEEE Antennas and Wireless Propagation Letters*, Vol. 17, No. 9, 1722–1726, 2018.

[21] Ur Rahman, S., H. Deng, M. I. Khan, N. Ullah, and Z. Uddin, "Integrated metasurface for efficient polarization conversion and high-gain, low-RCS EM radiation," *Optics Express*, Vol. 31, No. 17, 27 880–27 893, 2023.

[22] Zhu, H., J. Sun, and G. Xie, "A switchable linear-to-linear polarization converter with broadband performance," in *2022 International Applied Computational Electromagnetics Society Symposium (ACES-China)*, 1–2, Xuzhou, China, 2022.

[23] Wu, Y., S. Jia, and T. Zheng, "Design of an ultra-wide-angle reflective polarization conversion metasurfaces," in *2022 International Conference on Microwave and Millimeter Wave Technology (ICMMT)*, 1–3, Harbin, China, 2022.

[24] Lin, X., X. Zhang, M. Chang, W. Li, S. Yu, and M. Zhang, "Dual-band reflective polarization converter based on metasurface," *Optoelectronics Letters*, Vol. 19, 716–720, 2023.

[25] Guo, Y., J. Xu, C. Lan, and K. Bi, "Broadband and high-efficiency linear polarization converter based on reflective metasurface," *Engineered Science*, Vol. 14, No. 2, 39–45, 2021.